

# **Sensitivity study of solid fuel properties and dynamic behavior of pyrolysis in non-charring materials**

Sabarilal S, Ashruf Syed, Amit Kumar

National Centre for Combustion Research and Development & Department of Aerospace Engineering, Indian Institute of Technology Madras  
Chennai, Tamil Nadu, India

## **1 Introduction**

Pyrolysis modeling is complex since many of the input parameters are not known with high accuracy so there is a need for understanding the relative influence of material properties on pyrolysis process so that special care can be taken in experimentation to determine those parameters. Also the recent advances made the models more generalized and sophisticated yet all the physical processes were not captured. Lautenberger and Fernández-Pello[1] prescribed the material property estimation to be the focus owing to the challenges associated with determining the model inputs controlling the pyrolysis. In such cases, sensitivity study comes in handy as the pyrolysis which is the process under study has complex dependence on many parameters and underlying physical phenomena. Linteris[2] did a property variation study but a quantifiable sensitivity coefficient was not presented. Stoliarov et. al[3] and Chaos[4] applied the concept of sensitivity study to quantify the property variations, nevertheless external heat flux variation and thickness variation were not performed by the respective authors. This present study aims to provide additional information beyond aforementioned literature by considering the effect of thickness along with the variation of heat flux. Also it highlights the contribution of different physical phenomena happening during pyrolysis using Scaled Energy Balance (SEB) method.

Peak and average rate of heat release are commonly considered as key parameter characterizing polymer flammability[5]. To study about flame ignition, we need to invoke an ignition criterion for which the critical mass flux criterion was chosen as it is considered the most fundamental[6]. Also time to reach peak HRR determines the evacuation time. So for the present work, peak MLR, avg MLR,  $t_{ign}$  and time to peak MLR are considered as fire response parameters. Material sensitivity to these parameters is studied to quantify their relative influence.

Furthermore, the dynamic behavior of pyrolysis is studied using a SEB approach where the normalized contributions from each energy type viz. conduction, pyrolysis and transient term from the energy balance equation is analyzed to quantify the different physical processes within the material during pyrolysis. A combination of sensitivity study and dynamic analysis using SEB give a better understanding and physical insight into the process of pyrolysis.

## 2 Numerical Modeling

A 1D pyrolysis model coded in Fortran was used to predict the MLR of PMMA, and is validated against bench scale experiments by Chaos et. al [7]. A control volume approach is employed and the governing mass and energy conservation equations are solved numerically using a fully implicit scheme. In this present study only 2 species are treated virgin solid and pyrolysate. The decomposition of virgin solid to pyrolysate takes place through a single first order Arrhenius type endothermic reaction. Pyrolysis gas is assumed to be in thermal equilibrium with the solid and escape immediately once it is formed so that no pressure buildup within the solid. All properties in the model are taken to be temperature independent.

### a) Thermal Balance and Governing Equations

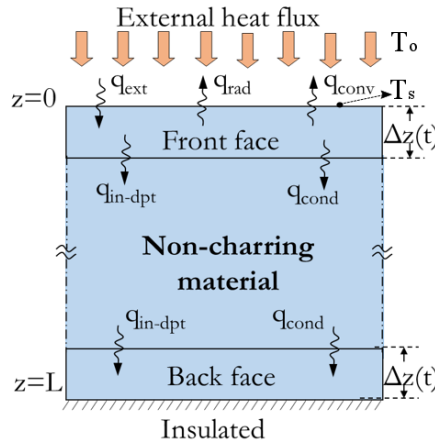


Figure 1. Schematic of thermal boundary condition for non-charring material

The mass and energy conservation equations for the solid phase are detailed in the Eq. (1) and (2). The pyrolysis rate of the sample is calculated by temperature depended Arrhenius equation presented in Eq. (3)

$$\frac{d\rho}{dt} = -\dot{m}''' \quad (1)$$

$$\frac{\partial(\rho C_p T)}{\partial t} = \frac{\partial}{\partial z} \left( k \frac{\partial T}{\partial z} \right) + \frac{\partial \dot{q}_r''}{\partial z} - \dot{m}''' H_p \quad (2)$$

$$\dot{m}''' = \frac{\partial m_i'''}{\partial t} = m_{i0}''' A e^{-\frac{E_a}{RT}} \left( \frac{m_i''}{m_{i0}''} \right)^n \quad (3)$$

Fig.3 shows the schematic of computational domain and boundary condition employed for the problem.

$$-k \frac{\partial T_{(0)}}{\partial z} = -h_c(T_s - T_o) - \varepsilon \sigma(T^4 - T_o^4) \quad (4)$$

$$k \frac{\partial T_{(L)}}{\partial z} = 0 \quad (5)$$

The front face boundary condition ( $z=0$ ) which includes conductive, radiative and convective term given by Eq.(4) whereas the bottom boundary( $z=L$ ) is taken as adiabatic given by Eq.(5). These are considered as standard boundary condition in bench scale experiments like FPA and cone calorimeter. In-depth absorption of external radiation is an important phenomenon for a translucent fuel like PMMA which is accounted by Eq.(6)

$$\frac{\partial \dot{q}_r''}{\partial z} = \eta \dot{q}_e'' e^{-\kappa z} (1 - e^{-\kappa \Delta z}) \quad (6)$$

### b) Experimental Validation

As seen from Fig. 2, even though the model is not able to exactly predict the position of peak MLR, it follows trend of the process, and reasonably accurate in predicting peak MLR. Table 1 represents model input parameters used from [7], except for transmissivity,  $\eta$  which is assumed to be equal to emissivity,  $\epsilon$ .

Table 1. Model input parameters (taken from [7])

Property	Value	Property	Value
$k$ (W/m/K)	0.191	$\kappa$ (m <sup>-1</sup> )	1716
$\rho$ (kg/m <sup>3</sup> )	1105	$A$ (s <sup>-1</sup> )	$3.98 \times 10^{11}$
$C_p$ (J/kg/K)	1507.1	$E_a$ (J/mol)	$1.62 \times 10^5$
$\epsilon$	0.837	$H_p$ (J/kg)	$7.37 \times 10^5$

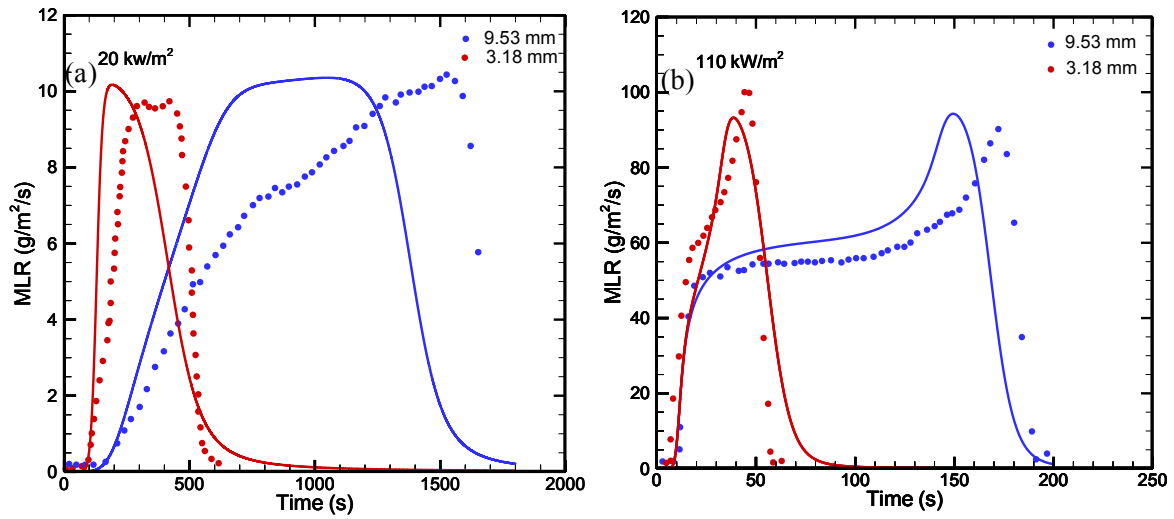


Figure 2. FPA MLR data for PMMA (symbols) compared to model results (lines) for different values of fuel thickness (3.18 mm and 9.53 mm) at different external heat fluxes of (a) 20kW/m<sup>2</sup> (b) 110kW/m<sup>2</sup>

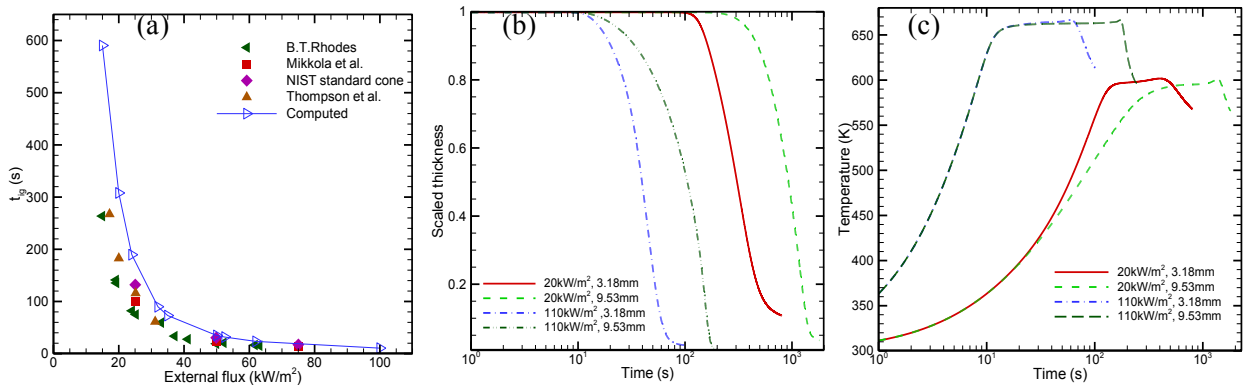


Figure 3. (a)  $t_{ign}$  as function of  $q_{ext}$ , comparison between numerical model prediction and different experimental results. (b) Scaled thickness and (c)  $T_{surface}$  profile as function of time for different initial thickness values subjected to different heat fluxes.

Fig. 3(a) compares the different experimental result and model predicting for ignition time verses external heat flux. For the present study, 3g/m<sup>2</sup>s is taken as the threshold MLR value, and the corresponding time

was defined as the ignition time  $t_{ign}$ . As seen from Fig. 3(a), even though the model is not able to predict the ignition time corresponding to lower heat fluxes, it follows trend of the process, and reasonably accurate in predicting the  $t_{ign}$  corresponding to higher heat fluxes. This shows the inefficiency of model to capture the physical phenomena happening in solid phase during lower heat flux. Since the model is following the same trend at low heat fluxes, the qualitative information made by this numerical model was felt to be reliable at these values. Fig. 3(b) and 3(c) corresponds to transient response of scaled thickness and surface temperature at different heat fluxes and specimen thickness.

### c) Time and grid independence study

The time and grid independence study of the model is summarized in Table 2. The parameters considered are peak MLR and time to peak MLR for two fuel thickness values viz. 3.18mm and 9.53mm. By considering the balance between accuracy and computation time, cell size of 0.05mm and time step of 0.05s are chosen for the simulation.

Table 2. Grid independence and time independence study

Time Independence Study					Grid Independence Study				
Cell thickness $\Delta x$ (mm)	Peak MLR (g/m <sup>2</sup> s)		Time to peak MLR (s)		Time step $\Delta t$ (s)	Peak MLR (g/m <sup>2</sup> s)		Time to peak MLR (s)	
	3.18mm	9.53mm	3.18mm	9.53mm		3.18mm	9.53mm	3.18mm	9.53mm
1.06	93.64	101.7	38.25	137.85	0.0025	93.47	94.52	38.66	149.20
0.636	93.41	96.30	38.45	146.15	0.005	93.45	94.51	38.67	149.21
0.318	93.28	94.68	38.60	148.4	0.01	93.43	94.48	38.37	149.23
0.1272	93.24	94.35	38.65	149.2	0.02	93.38	94.43	38.66	149.28
0.0636	93.24	94.30	38.65	149.35	0.05	93.24	94.28	38.65	149.40
0.0318	93.24	94.29	38.65	149.4	0.1	93.00	94.04	38.70	149.60
0.0159	93.24	94.28	38.65	149.4	0.2	92.52	93.55	38.60	150.00
0.0106	93.24	94.28	38.65	149.4	0.4	91.59	92.6	38.80	150.80

## 3 Sensitivity Study of Fire Response Parameters

### a) Methodology

$$s_{i,j} = \frac{(\Delta f / f_0)}{(\Delta p / p_0)} \quad (7)$$

Sensitivity coefficient of an output 'f' to a given input 'p' at the base values ( $p_0$ ,  $f_0$ ) is defined by Eqn. (7), where  $\Delta f$  and  $\Delta p$  are the respective perturbations in f and p from the base values. For the present analysis, input parameter refers to one of the solid fuel properties, and the output refers to one of the fire response parameters. Also as seen from Eqn. (7),  $s_{i,j}$  was defined as a non-dimensional value which allowed us to compare the sensitivities of any output to any input, even for different fire environments characterized by the external heat fluxes.

Sensitivity was evaluated for each combination of f and p by taking the PMMA properties[7] as the base value, and as an average value obtained by perturbing the input parameter by  $\pm 1\%$  of base value. Therefore to span the analysis for all the 4 output and 8 input parameters, with 2 external heat flux and 2 thickness values, a total of 256 such cases were executed. Also to be noted that  $E_a/\ln(A)$  term was taken as a single parameter as suggested in [2]–[4] to account for the underlying kinetic-compensation effect[8]

### b) Results and discussions

Fig. 4 shows the sensitivity of all the fire response parameters considered to the material properties for the non-charring material. For sensitivity plot shown here, the positive value indicates that increasing the

input parameter results in an increase in output variable and vice versa. And the magnitude of the coefficient reflects the influence of material property on the fire parameters.

On a global comparison, it can be seen that the maximum sensitivity values mostly occur at 20 kW/m<sup>2</sup>. This can be attributed to slow reactions at low heat fluxes. Since the specimen under consideration is optically translucent, as expected, the sensitivity of any parameter to  $\eta$  is high irrespective of thickness and heat flux. To point out specific comparisons with the literature, effect of  $\kappa$  on  $t_{\text{ign}}$  is higher at high heat flux which is in compliance with Jiang et. al[9] and Bal and Rein[10]. Also the qualitative behavior of sensitivity coefficients is in well-agreement with that of Stoliarov et. al[3] and Marcos[4]

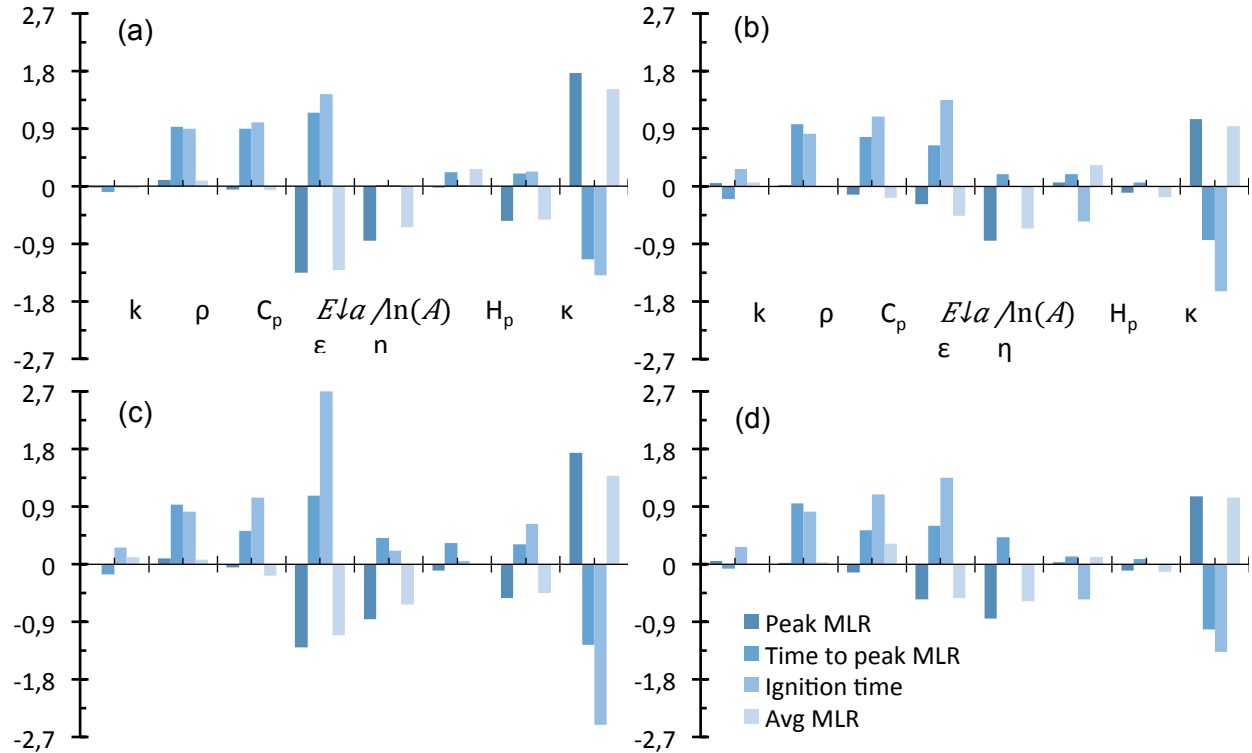


Figure 4. Sensitivity coefficients of fire response parameters (Peak MLR, Time to Peak MLR, Ignition time, and Avg MLR) subjected to solid fuel properties ( $k$ ,  $\rho$ ,  $C_p$ ,  $E_a/\ln A$ ,  $H_p$ ,  $\kappa$ ,  $\epsilon$ , and  $\eta$ ) for different external heat flux and specimen thickness values: (a) 20 kW/m<sup>2</sup>, 3.18 mm (b) 100 kW/m<sup>2</sup>, 3.18 mm (c) 20 kW/m<sup>2</sup>, 9.53 mm (d) 110 kW/m<sup>2</sup>, 9.53 mm.

#### 4 Dynamic Analysis of Pyrolysis using Scaled approach

##### a) Methodology

The entire process of pyrolysis is unsteady which is evident from all the previous analysis carried starting from Fig. 2 through Fig. 4. A further closer look at Eqn. (2) governing the physical phenomena of the process gave us the idea of studying different energy contribution at various time stamp, heat flux and thickness values. As mentioned earlier, due to the translucence, the effective energy used by the material is from the in-depth absorption unlike other opaque and/or charring materials where the entire energy absorption happens at the exposed surface layer later heating the material through conduction. So for studying the dynamics of pyrolysis with the help of energy balance, it was logical to normalize each of the energy contribution using the  $q_{\text{in-dpt}}$  given by Eqn.(6), and the whole analysis is termed as Scaled-Energy Balance (SEB) approach.

### b) Results and discussion

Conduction, pyrolysis and transient (which is used for the temperature rise) terms are the three contributions to the SEB analysis. Dynamics of these scaled energies integrated over the thickness of the specimen are plotted in Fig. 5 for the set of heat flux and thickness values taken for the previous study. Note that in Fig. 5 the SEB approach is valid only for the LHS of the dotted vertical line beyond which (on RHS) the material becomes thinner, and where a large part of  $q_{in-dpt}$  is not absorbed which reduces the heating rate (transient energy term) of material. It can also be seen in Fig. 3(c) where the temperature starts dropping beyond this point.

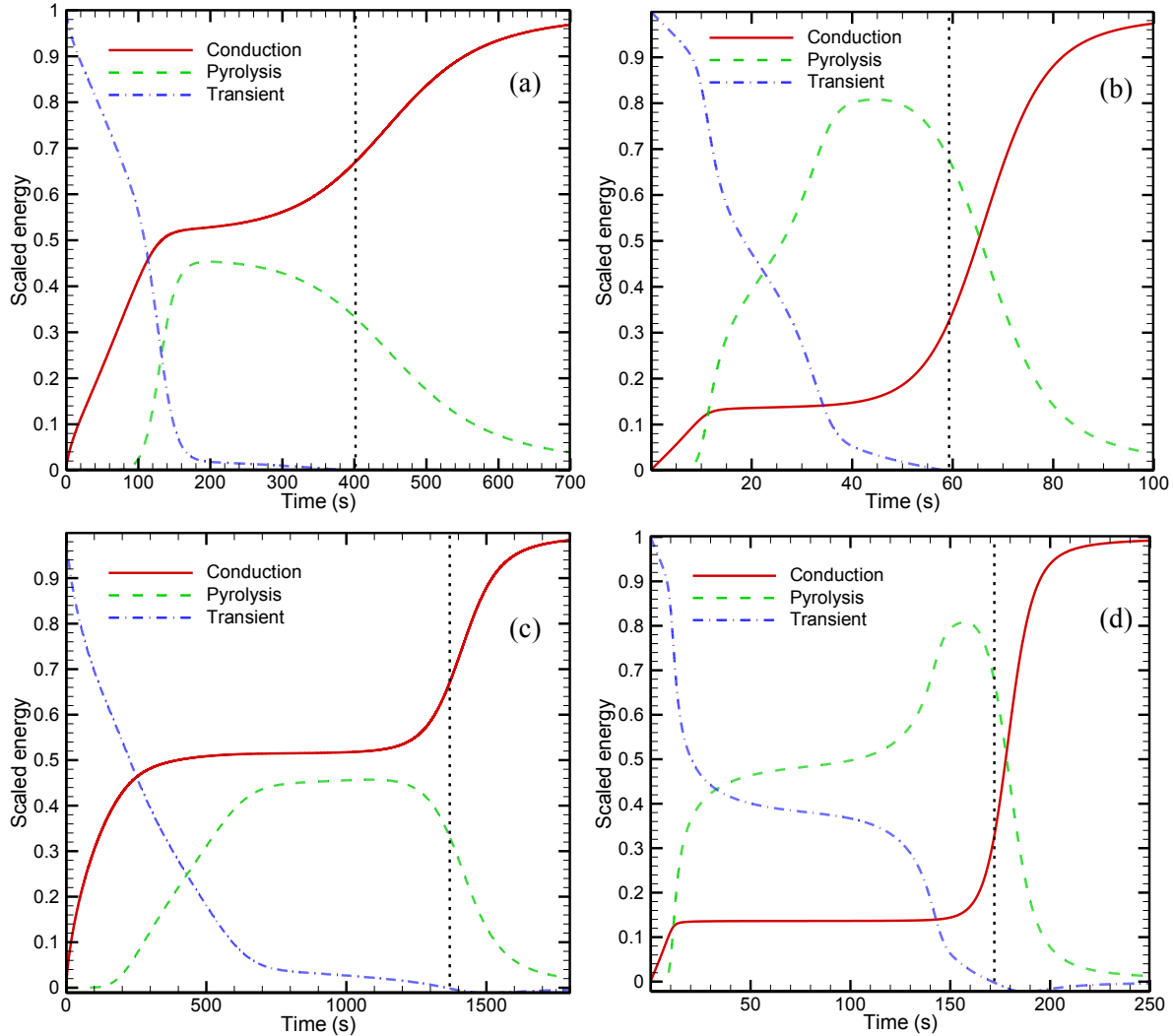


Figure 5. Dynamics of Pyrolysis plotted with scaled contributions of Conduction, Pyrolysis and Transient terms using SEB approach for different external heat flux and specimen thickness values: (a) 20 kW/m<sup>2</sup>, 3.18 mm (b) 100 kW/m<sup>2</sup>, 3.18 mm (c) 20 kW/m<sup>2</sup>, 9.53 mm (d) 110 kW/m<sup>2</sup>, 9.53 mm

The consistent sensitivity of  $\rho$  and  $C_p$  to  $t_{ign}$  can be well explained from the above SEB dynamic plots. Since the thermal energy is getting into the solids, primarily through in-depth absorption, the thermal conductivity has less contribution in pyrolysis as compared to  $\rho$  and  $C_p$ . At lower heat flux, the energy reaching in-depth of the specimen will be lower and therefore pyrolysis reaction gets delayed, and

conduction dominates in the early stages. In contrast to this, for high heat flux where sufficient energy is present for both processes, pyrolysis dominates since the reaction time scales are small compared to conduction. Also energy used for pyrolysis follows the corresponding trends of MLR reported in Fig. 2

## 5 Concluding Remarks

Transient MLR for non-charring polymer at different heat flux and thickness has been predicted numerically. To get more insight into global fire behavior of materials, 4 fire response parameters have been chosen based on the previous literature and the sensitivity of 8 material properties to fire response parameter are studied. The sensitivity results obtained agree qualitatively well with previous works. Fire properties show high sensitivity to  $\eta$  and  $E_a/\ln(A)$ . Effect of thickness and  $q_{ext}$  on sensitivity coefficient is obtained. It was observed that thicker materials subjected to lower heat flux are more sensitive due to the slow reactions.

For the dynamic analysis, SEB approach was adopted to get the understanding of transient energy balance during pyrolysis. From the results, the inference from various energy contributions was used to explain the pyrolysis delay under lower heat flux conditions, and also the consistent sensitivity of  $\rho$  and  $C_p$  irrespective of heat flux and thickness. A combination of both sensitivity study and dynamics of pyrolysis will give more understanding in development and interpretation of fire-retardant materials in general, with possible applications in fire safety studies.

Nonetheless, the present study did not account for the back reflection assuming the back surface to be fully transparent which affects the thermal balance during the intermediate phase of pyrolysis. Radiation effects of the surface apart from in-depth absorption was not considered which is the reason for reducing heating rate of material further resulting in the drop of surface temperature which is not realistic. Other physical phenomena contributing to the energy balance including, but not limited to bubbling, temperature dependent properties, in-depth emission etc., can be included in the model for a more pragmatic approach.

## Nomenclature

$\kappa$	Radiative absorption coefficient	$A$	Pre-exponential factor
$\dot{m}'''$	Reaction rate per unit volume	$E_a$	Activation energy
$\dot{q}_e''$	External heat flux	$R$	Universal gas constant
$\rho$	Density	$z$	Depth into the sample
$\sigma$	Stefan-Boltzmann constant	$\varepsilon$	Emissivity
$\eta$	Transmissivity	$h_c$	Convective heat transfer coefficient
$H_p$	Heat of reaction	$t_{ig}$	Ignition time
$k$	Thermal conductivity	$MLR$	Mass Loss Rate
$C_p$	Specific heat	$LHS$	Left Hand Side
$T$	Temperature	$RHS$	Right Hand Side

## 6 References

- [1] C. W. Lautenberger and A. C. Fernandez-Pello, "Generalized pyrolysis model for combustible solids," *Fire Saf. J.*, vol. 44, no. 6, pp. 819–839, 2009.
- [2] G. T. Linteris, "Numerical simulations of polymer pyrolysis rate: Effect of property variations," *Fire Mater.*, vol. 35, no. 7, pp. 463–480, Nov. 2011.
- [3] S. I. Stoliarov, N. Safronava, and R. E. Lyon, "The effect of variation in polymer properties on the rate of burning," *Fire Mater.*, vol. 33, no. 6, pp. 257–271, Oct. 2009.
- [4] M. Chaos, "Application of sensitivity analyses to condensed-phase pyrolysis modeling," *Fire Saf.*

- J.*, vol. 61, pp. 254–264, Oct. 2013.
- [5] P. Di Nanno (Ed.), *SFPE Handbook of Fire Protection Engineering*, Third. Quincy, MA: National Fire Protection Association, 2002.
  - [6] D. Drysdale, *An Introduction to Fire Dynamics*. Chichester, UK: John Wiley & Sons, Ltd, 2011.
  - [7] M. Chaos, M. M. Khan, N. Krishnamoorthy, J. L. de Ris, and S. B. Dorofeev, “Evaluation of optimization schemes and determination of solid fuel properties for CFD fire models using bench-scale pyrolysis tests,” *Proc. Combust. Inst.*, vol. 33, no. 2, pp. 2599–2606, Jan. 2011.
  - [8] A. V. Nikolaev, V. A. Logvinenko, and V. M. Gorbachev, “Special features of the compensation effect in non-isothermal kinetics of solid-phase reactions,” *J. Therm. Anal.*, vol. 6, no. 4, pp. 473–477, Jul. 1974.
  - [9] F. Jiang, J. L. de Ris, and M. M. Khan, “Absorption of thermal energy in PMMA by in-depth radiation,” *Fire Saf. J.*, vol. 44, no. 1, pp. 106–112, 2009.
  - [10] N. Bal and G. Rein, “Numerical investigation of the ignition delay time of a translucent solid at high radiant heat fluxes,” *Combust. Flame*, vol. 158, no. 6, pp. 1109–1116, 2011.

## 7 Response to Reviewers’ comments

\* Comments: RHS and LHS should be included in the Nomenclature. Rather than giving details (table) of the sensitivity study, I would recommend that you give the model input parameters in 2b. conductivity, emissivity, absorbance,  $h_c$ ,  $c_p$ ,  $E_a$ ..... otherwise the reader has to read [6] in addition to have all the data for your paper. What is the value for  $H_p$ ? Add  $T_o$  and  $T_s$  to Figure 1. Equation 6, wrong letter for absorptivity.

All these comments have been considered and corrected wherever required.

Q1: The model you are using is very simple; no temperature dependent property, single order Arrhenius, no mass transport in the solid, 1D, but agrees surprisingly well with the experiments. Is this due to parameter adjustment or is the physics/chemistry so simple that the neglected effects do not play a significant role?

A1: Yes, as pointed out by the reviewer, the present work is just a preliminary study to understand sensitivity of model input parameters for pyrolysis process in non-charring materials. And the data matches well with the experiments because the values used as input parameters for solid fuel properties are optimized values (obtained by parameter adjustment as employed in [7]). Nonetheless only  $A$  and  $E_a$  are artificial properties, and the rest of them are within the range of actual physical properties of PMMA.

Q2. Why is the model not able to predict the measurements accurately at lower heat fluxes? I would recommend to add a comment on my remark.

A2. As pointed out in section 3(b), and when observed in Figure 4, the MLR is more sensitive to input parameters at low heat fluxes. This can be attributed to slow reactions at low heat fluxes. Considering the temperature dependency and transient variation of these parameters in the analysis might resolve this mismatch.

Q3. I am not sure whether I understand Figure 5. The difference of the curves should be  $dq_r/dz$



according to equation 2, correct?, if so mention it? Shouldn't the energy balance be a function of the z coordinate, because the Temperature is a function of z and hence, for example, heat of pyrolysis? So the question is then what is the z coordinate for Figure 5? However, it might be that I misunderstand Figure 5

A3. Figure 5 represents different contributions in the energy balance which are integrated over thickness of the specimen. And the dynamic analysis means the scaled energy contributions are presented over time. So as pointed out by the reviewer, the plot is not a function of z coordinate, rather a function of time for a given thickness.